International Conference Mathematical and Computational Biology 2011
International Journal of Modern Physics: Conference Series
Vol. 9 (2012) 178–192

DOI: 10.1142/S2010194512005247

NUMERICAL COMPUTATION OF A TWO-DIMENSIONAL BIOMAGNETIC CHANNEL FLOW

NURSALASAWATI RUSLI

Institute of Engineering Mathematics,
Universiti Malaysia Perlis,
02000 Kuala Perlis, Perlis, Malaysia
nursalasawati@unimap.edu.my

AHMAD KUEH BENG HONG, ERWAN HAFIZI KASIMAN and AIRIL YASREEN MOHD YASSIN

Steel Technology Centre, Faculty of Civil Engineering,
Universiti Teknologi Malaysia, 81310 Skudai, Johor
kbhahmad@utm.my, erwanhafizi@utm.my, ayasreen@utm.my

NORSARAHAIDA AMIN

Department of Mathematics, Faculty of Science,
Universiti Teknologi Malaysia, 81310 Skudai, Johor
norsarahaida@utm.my

The present paper studies the fundamental problem of the biomagnetic fluid flow in a channel under the influence of a spatially varying magnetic field. The solution of the problem is obtained using an improved finite difference method. This approach has successful handled the pressure of the flow which is the main problem in the finite difference method. Results concerning the velocity indicates that the presence of magnetic field appreciably influence the flow field. A distortion in terms of asymmetric flow profile was observed near the magnetic source. Also a vortex is demonstrated near the lower plate where the magnetic source is placed.

Keywords: Magnetic field; biofluid; finite difference method; staggered grid.

1. Introduction

Biomagnetic fluid dynamics (BFD) is the study of the interaction of biological fluids with an applied magnetic field. The study of the BFD flow has been investigated by several researchers for numerous applications in bioengineering and medicine. Among them are the development of magnetic devices for cell separation, targeted transport of drugs i.e. using magnetic particles as drug carriers, magnetic wound treatment and cancer tumor treatment causing magnetic hyperthermia.[1-3] Very encouraging findings have been reported in the clinical application of magnetic drug targeting (MDT) in loco-regional cancer treatment.[4-6] The computational simulations[7,8] revealed a significant potential for applying MDT to the treatment of atherosclerosis.

We believe that mathematical modelling and numerical simulations provide many important insights into the interactions between blood flow and magnetic field. Computational simulations make possible the study of the feasibility of a medical technique before entering clinical trials, and simulations are useful for investigating the influence of various factors independently.[9] Since the human blood is slightly electrically conductive, it is important to formulate a mathematical model that take into account the effect of magnetisation and Lorentz force on the blood flow.

In order to examine the flow of a BFD, mathematical models have been developed in Ref. 1. The BFD model is based on the Ferrohydrodynamics (FHD),[10] which deals with non-inducing electric current and considers that the flow is affected by the magnetisation of the fluid in the magnetic field.[11] For a full description of a blood flow, the contribution of the Lorentz force due to the induced electric current of Magnetohydrodynamic (MHD)[12] should be taken into account. Therefore, an extended BFD mathematical model, which includes the Lorentz force was developed in Ref. 11. The model was extended where the electric potential term was included in the expression of the total current density.[13] The author prescribed the additional effect because experiments[14,15] have shown that an imposed magnetic field alternated the electrocardiogram (ECG) of the human cardiac rhythm, indicating the significance of the induced voltages.

From literature there are several methods considered in solving biomagnetic fluid flow using numerical method. The stream function–vorticity formulation[16] was adopted for the numerical investigation of the steady fluid flow in a channel under the influence of a spatially varying magnetic field. The development of a more stable and simpler technique in the application for BFD problems was presented in Ref. 17. The technique was used to investigate the flow in a channel with symmetric stenosis.[18] Finite analytic method[19] was used for the simulation of flow in a channel with thrombus while the finite volume method[20] was used to simulate a biomagnetic fluid in a stenotic artery.

In the present study, the Finite Difference Method (FDM) will be adopted. One of the main challenges of using the FDM is in the handling of the pressure of the flow. To overcome this problem, a new scheme that is implemented with the SIMPLE-type algorithm for the pressure field calculation is proposed.[21] The nonlinear partial differential governing equations will be discretised using the finite difference approximation which is carried out in a staggered grid. The advantages of using the staggered grid over a non-staggered grid are twofold. First, the continuity equation can be written at node i,j with the central difference up to a second order accuracy without the interpolation of the relevant velocity components. Second, it prevents the odd-even coupling or what is known as the checkerboarding between the pressure and the velocity fields.[22]

However, the formulation[21] is devised for the Navier-Stokes equations only. Therefore, this paper aims to provide a modified scheme that handles the additional magnetic part. We will present the formulation of the scheme and the simulation of a biomagnetic fluid flow based on the new model. First, the governing equations and the boundary conditions are presented in Section 2. Then, section 3 discusses the new scheme in details while the validation of this method is shown in section 4. Finally, section 5 presents the numerical simulation of a biomagnetic fluid flow under the influence of a spatially varying magnetic field.

2. Governing Equations

In the present study, the steady, two-dimensional, incompressible and laminar flow is considered. The energy equation is not considered in this paper i.e. isothermal case. The contribution of the Lorentz force due to the MHD is not taken into account.

The governing equations of the fluid flow, under the influence of a spatially varying magnetic field are given as[16]:

continuity equation

$$\frac{\partial u^*}{\partial x^*} + \frac{\partial v^*}{\partial y^*} = 0 \tag{1}$$

x-momentum equation

$$u^* \frac{\partial u^*}{\partial x^*} + v^* \frac{\partial u^*}{\partial y^*} = -\frac{1}{\rho^*}\frac{\partial p^*}{\partial x^*} + \nu^* \left(\frac{\partial^2 u^*}{\partial x^{*2}} + \frac{\partial^2 u^*}{\partial y^{*2}} \right) + \frac{\mu_0{}^* M^*}{\rho^*}\frac{\partial H^*}{\partial x^*} \tag{2}$$

y-momentum equation

$$u^* \frac{\partial v^*}{\partial x^*} + v^* \frac{\partial v^*}{\partial y^*} = -\frac{1}{\rho^*}\frac{\partial p^*}{\partial y^*} + \nu^* \left(\frac{\partial^2 v^*}{\partial x^{*2}} + \frac{\partial^2 v^*}{\partial y^{*2}} \right) + \frac{\mu_0{}^* M^*}{\rho^*}\frac{\partial H^*}{\partial y^*} \tag{3}$$

The boundary conditions are

$$x^* = 0 \text{ or } x^* = L^* \text{ and } 0 \le y^* \le L^*: \; u^* = v^* = 0,$$
$$y^* = 0 \text{ or } y^* = L^* \text{ and } 0 \le x^* \le L^*: \; u^* = v^* = 0,$$

where u and v are the velocity components in the x and y directions respectively, p is the pressure, ρ is the constant density, $\nu^* = \mu^* / \rho^*$ is the kinematic viscosity, μ_0 is magnetic permeability in vacuum, M^* is the magnetisation and H^* is the magnetic field

intensity. The variation of the magnetic field is at the $x^* - y^*$ plane, so the magnetic terms on the right hand side in Eqs. (2) and (3) represent the magnetisation force per unit mass in the x^* and y^* directions, respectively.

The magnetisation equation for isothermal case is given by

$$M = \chi H \tag{4}$$

where χ is the magnetic susceptibility constant.

The effect of magnetic field can only influence the solution of the problem if the magnetic field intensity, H is spatially varying. For constant value of H, the first derivative of H in Eqs. (2) and (3) render the magnetic product to null and we have our basic momentum equations.

Using the dimensionless definitions as given below[16, 23]:

$$x = \frac{x^*}{h},\ y = \frac{y^*}{h},\ u = \frac{u^*}{U},\ v = \frac{v^*}{U},\ p = \frac{p^*}{\rho U^2},\ H = \frac{H^*}{H_0}.$$

the governing equations (1) to (3) become

$$\frac{\partial u}{\partial x} + \frac{\partial v}{\partial y} = 0 \tag{5}$$

$$u\frac{\partial u}{\partial x} + v\frac{\partial u}{\partial y} = -\frac{\partial p}{\partial x} + \frac{1}{\mathrm{Re}}\left(\frac{\partial^2 u}{\partial x^2} + \frac{\partial^2 u}{\partial y^2}\right) + \frac{Mn_F}{\mathrm{Re}} H \frac{\partial H}{\partial x} \tag{6}$$

$$u\frac{\partial v}{\partial x} + v\frac{\partial v}{\partial y} = -\frac{\partial p}{\partial y} + \frac{1}{\mathrm{Re}}\left(\frac{\partial^2 v}{\partial x^2} + \frac{\partial^2 v}{\partial y^2}\right) + \frac{Mn_F}{\mathrm{Re}} H \frac{\partial H}{\partial y} \tag{7}$$

and the boundary conditions are

$$x = 0 \ \text{ or } \ x = 1 \ \text{ and } \ 0 \le y \le 1: \ \ u = v = 0,$$

$$y = 0 \ \text{ or } \ y = 1 \ \text{ and } \ 0 \le x \le 1: \ \ u = v = 0.$$

Here, $\mathrm{Re} = \dfrac{h^* \rho^* u_r^*}{\mu^*}$ is the Reynolds number and $Mn_F = \dfrac{B_0^{*2} \chi h^*}{U \rho^* \mu_0 \nu}$ is the magnetic number.

3. Numerical Method

The solution of the governing equations presented in the previous section, Eqs. (5)-(7) is essentially based on a new numerical algorithm[21] with additional treatment on the magnetic terms. Also, there are some modifications in the discretisation of the Navier-Stokes equations which will be explained in a later section. The convective terms in the momentum equations are approximated using the first or second order finite difference formulae. An equally spaced grid points are chosen in this study for the handling of *u*- and *v*-momentum equations at the wall boundary, whereas unequally spaced grid points have been used for the same nodes.[21]

3.1. *Finite differencing on a staggered grid*

Consider a two-dimensional rectangular domain as shown in Figure 1. The domain is discretised using a regular Cartesian mesh. The mesh is uniform in each of the x and y directions. A staggered grid is used to store the velocity components u and v and the pressure p.

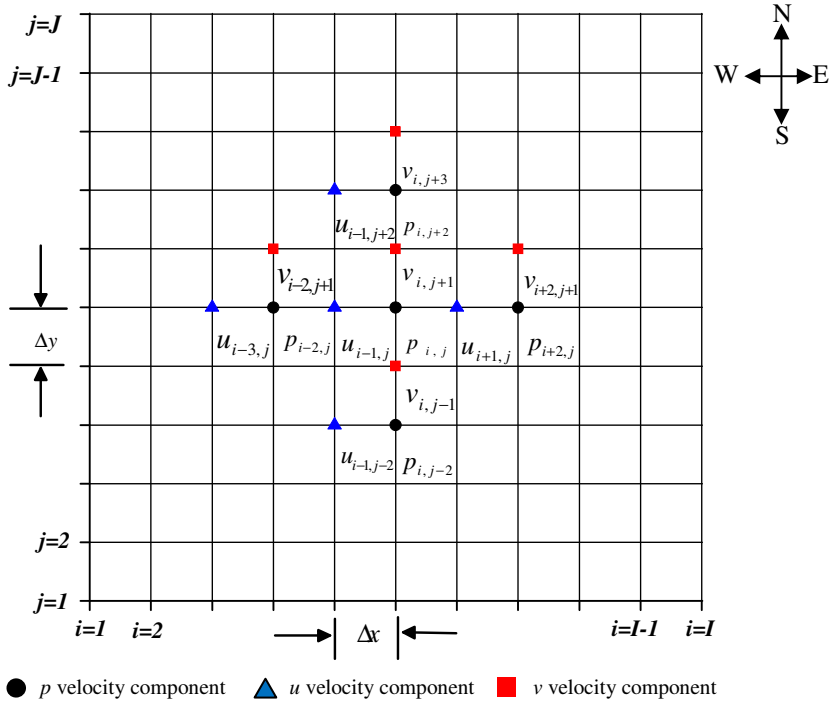

Figure 1: Staggered grid arrangement.

As indicated in Figure 1, for point *i*, *j*, the values of *u* and *v* are stored at the *i-1,j* and *i,j+1* locations respectively and *p* is stored at *i,j*. Thus, the *u*-momentum equation, Eq. (6) is discretised at *i-1,j*, the *v*-momentum equation, Eq. (7) at *i,j+1*, and the continuity equation (5) at *i,j*. Here, a first-order upwind differencing scheme is used to approximate the convective terms in the momentum equations, while a second-order central differencing is used for the diffusion terms. The pressure gradients are approximated by a second order central difference scheme. Due to the fact that the magnetic field intensity *H* acts as body force to our systems, the calculation of magnetic field intensity *H* from the momentum equations was treated to be the same as pressure *p*. Furthermore, because the values of $H\frac{\partial H}{\partial x}$ and $H\frac{\partial H}{\partial y}$ from Eqs. (6) and (7) are known, they can be evaluated in prior at each node.

3.2. *Discretisation of the momentum equations*

Unequally spaced grid points[21] have been used for the handling of *u*- and *v*- momentum equations at the wall boundary, i.e. the convective term is approximated using a second order accurate expression while the diffusion term takes the first order accurate expression. It hence leads to a set of formulae with different order at different node location. Alternatively, equally spaced grid points are chosen in this study. Discretisation of the *u*- and *v*- momentum equations at interior nodes can be used at the wall boundary. The discretisation of the momentum equations can be summarized as below.

3.2.1. *u-momentum equation*

The discrete *u*-momentum equations at interior nodes are given by

$$a_P^{\text{int}} u_{i-1,j} + a_N^{\text{int}} u_{i-1,j+2} + a_S^{\text{int}} u_{i-1,j-2} + a_W^{\text{int}} u_{i-3,j} + a_E^{\text{int}} u_{i+1,j} = \frac{\hat{p}_{i-2,j} - \hat{p}_{i,j}}{2\rho\Delta x} + Mn_F H\frac{\Delta H_{i,j}}{\Delta x}$$

where

$$a_P^{\text{int}} = \frac{\hat{u}_{i-1,j}}{2\Delta x} + \nu\left(\frac{1}{2\Delta x^2} + \frac{1}{2\Delta y^2}\right)$$

$$a_N^{\text{int}} = \frac{\hat{v}_{i-1,j}}{4\Delta y} - \frac{\nu}{4\Delta y^2}$$

$$a_S^{\text{int}} = -\frac{\hat{v}_{i-1,j}}{4\Delta y} - \frac{\nu}{4\Delta y^2}$$

$$a_W^{\text{int}} = -\frac{\hat{u}_{i-1,j}}{2\Delta x} - \frac{\nu}{4\Delta x^2}$$

$$a_E^{\text{int}} = -\frac{\nu}{4\Delta x^2}$$

The caret above a variable indicates the quantities that will be calculated at the previous iteration. Because of the use of a staggered grid, the values of v in the u-momentum equation and u in the v-momentum equation, appearing as the coefficients of the convective derivatives, are not available at the desired points.

Therefore, these velocities are computed to a second order accuracy using four surrounding grid points at which they are stored,

$$u\big|_{i,j+1} = \frac{u_{i+1,j} + u_{i+1,j+2} + u_{i-1,j} + u_{i-1,j+2}}{4}$$

$$v\big|_{i-1,j} = \frac{v_{i,j-1} + v_{i,j+1} + v_{i-2,j-1} + v_{i-2,j+1}}{4}$$

The discrete u-momentum equations at boundary nodes are the same as interior node with some modifications. For example, the discrete u-momentum equations at the inlet nodes is the same as interior node except that the value of $u_{1,j}$ is known. The u-momentum equation along the bottom of the wall $(j=2)$ takes the form

$$a_P^S u_{i-1,2} + a_N^S u_{i-1,4} + a_W^S u_{i-3,2} + a_E^S u_{i+1,2} = \frac{\hat{p}_{i-2,2} - \hat{p}_{i,2}}{2\rho\Delta x} + \left(\frac{2\nu}{3\Delta y^2} + \frac{2v_{i-1,2}}{3\Delta y}\right) u_{i-1,1} + Mn_F H \frac{\Delta H_{i,2}}{\Delta x}$$

where

$$a_P^S = \frac{\hat{u}_{i-1,2}}{2\Delta x} + \frac{\hat{v}_{i-1,2}}{2\Delta y} + \nu\left(\frac{1}{2\Delta x^2} + \frac{1}{2\Delta y^2}\right)$$

$$a_N^S = \frac{\hat{v}_{i-1,2}}{6\Delta y} - \frac{\nu}{3\Delta y^2}$$

$$a_W^S = -\frac{\hat{u}_{i-1,2}}{2\Delta x} - \frac{\nu}{4\Delta x^2}$$

$$a_E^S = -\frac{\nu}{4\Delta x^2}$$

In a refined form, the current method presents the u-momentum equation along the bottom of the wall as

$$a_P^{\text{int}} u_{i-1,2} + a_N^{\text{int}} u_{i-1,4} + a_W^{\text{int}} u_{i-3,2} + a_E^{\text{int}} u_{i+1,2} = \frac{\hat{p}_{i-2,2} - \hat{p}_{i,2}}{2\rho\Delta x} - a_S^{\text{int}} u_{i-1,1} + Mn_F H \frac{\Delta H_{i,2}}{\Delta x}$$

Here, all other coefficients are the same as defined at the interior nodes.

3.2.2. *v-momentum equation*

The discrete *v*-momentum equations at the interior nodes take the following form

$$b_P^{\text{int}} v_{i,j+1} + b_N^{\text{int}} v_{i,j+3} + b_S^{\text{int}} v_{i,j-1} + b_W^{\text{int}} v_{i-2,j+1} + b_E^{\text{int}} v_{i+2,j+1} = \frac{\hat{p}_{i,j} - \hat{p}_{i,j+2}}{2\rho\Delta y} + Mn_F H \frac{\Delta H_{i,j}}{\Delta y}$$

where

$$b_P^{\text{int}} = \frac{\hat{u}_{i,j+1}}{2\Delta x} + \nu\left(\frac{1}{2\Delta x^2} + \frac{1}{2\Delta y^2}\right)$$

$$b_N^{\text{int}} = \frac{\hat{v}_{i,j+1}}{4\Delta y} - \frac{\nu}{4\Delta y^2}$$

$$b_S^{\text{int}} = -\frac{\hat{v}_{i,j+1}}{4\Delta y} - \frac{\nu}{4\Delta y^2}$$

$$b_W^{\text{int}} = -\frac{\hat{u}_{i,j+1}}{2\Delta x} - \frac{\nu}{4\Delta x^2}$$

$$b_E^{\text{int}} = -\frac{\nu}{4\Delta x^2}$$

3.3. *Discretisation of the continuity equation*

The pressure correction equations for all boundary nodes are identical to Ref. 21. The pressure correction equations for the interior nodes are

$$c_P^{\text{int}} p'_{i,j} + c_E^{\text{int}} p'_{i+2,j} + c_W^{\text{int}} p'_{i-2,j} + c_N^{\text{int}} p'_{i,j+2} + c_S^{\text{int}} p'_{i,j-2} = \frac{u^*_{i-1,j} - u^*_{i+1,j}}{2\Delta x} - \frac{v^*_{i,j+1} - v^*_{i,j-1}}{2\Delta y}$$

where

$$c_P^{\text{int}} = \frac{1}{4\rho\Delta x^2 a_{i+1,j}} + \frac{1}{4\rho\Delta x^2 a_{i-1,j}} + \frac{1}{4\rho\Delta y^2 b_{i,j+1}} + \frac{1}{4\rho\Delta y^2 b_{i,j-1}}$$

$$c_E^{\text{int}} = -\frac{1}{4\rho\Delta x^2 a_{i+1,j}}$$

$$c_W^{\text{int}} = -\frac{1}{4\rho\Delta x^2 a_{i-1,j}}$$

$$c_N^{\text{int}} = -\frac{1}{4\rho\Delta y^2 b_{i,j+1}}$$

$$c_S^{\text{int}} = -\frac{1}{4\rho\Delta y^2 b_{i,j-1}}$$

The equations for pressure correction p' at boundary nodes are the same as the interior nodes with some modifications.

3.4. *Solution algorithm*

For the current study, the SIMPLE scheme is employed for the pressure-velocity coupling in the overall solution. The procedure can be summarised in the following steps:

i) Start with an initial pressure field p^*.
ii) Solve the momentum equations to obtain the intermediate velocity components U^*, V^*.
iii) Solve the pressure-correction equation to obtain the pressure correction p'.
iv) Update the intermediate pressure and velocity fields with the corrected values $p = p^* + p'$, $U = U^* + U'$, $V = V^* + V'$
v) Take the newly corrected pressure p as a new initial pressure p^* and repeat the entire procedure until a fully convergent solution is obtained.

Note that the pressure-correction equation is also prone to divergence unless an under-relaxation is implemented. For a such purpose, the following is used.

$$p = p^* + \alpha_P p' \tag{8}$$

Here, α_P is the pressure under-relaxation parameter which is set to 0.7.

Tri-Diagonal Matrix Algorithm (TDMA)[21] is used to solve the system of discretised equations. The TDMA is applied line by line to solve for u, v, and p and the solution is iterative. The algorithm sweeps once from left to right across the grid to solve for u, v, and p. However, this algorithm takes a considerable long time to converge. In the present algorithm, a modification in the form of a direct method is made to remedy the problem. It has been shown that a rapid convergence can be achieved through this method.[24]

4. Test Problem

The developed finite difference formulation is applied to a well-established benchmark problem, namely, the developing laminar flow in a straight rectangular duct. Note that the magnetic terms are not included here. This problem is considered merely for the validation of our present model.

4.1. *Developing flow in a rectangular duct*

Consider a developing flow in a straight two-dimensional channel as shown in Figure 2. The length *L* of the channel is taken to be ten times the width *D*, and we take $D=1$.

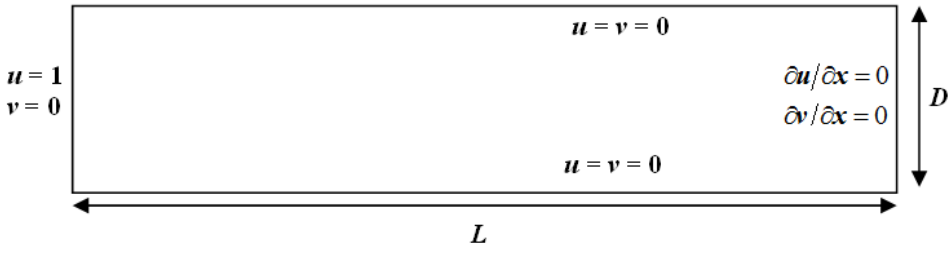

Figure 2: Geometry of the channel with the prescribed boundary conditions.

At the entrance of the channel, a uniform flow $(u=1)$ is specified as the inlet velocity profile. The transverse velocity is set equal to zero at the inlet. A parallel flow condition is specified at the outlet, i.e. $\partial u/\partial x=0$ and $\partial v/\partial x=0$. The no-slip condition is applied at the lower and upper walls. As the fluid enters the channel, the wall boundary conditions distort the uniform flow as boundary layers grow on the walls. The flow develops along the channel for some distance, until it becomes fully developed. At this point, the flow field is that described by the Poiseuille flow.

The numerical model is verified against the exact solution[25] and Zogheib model[21] for a fully developed flow formed at the outlet. Also, the predicted fully developed streamwise velocity profile for $\mathrm{Re}=50$ is compared and the agreement is excellent, as given in Figure 3. In Figure 4, the result obtained for the present method closely match the result from Ref. 21 and the agreement is better than that obtained from Ref. 25 where the parabolic profile starts further downstream, around $x=4$.

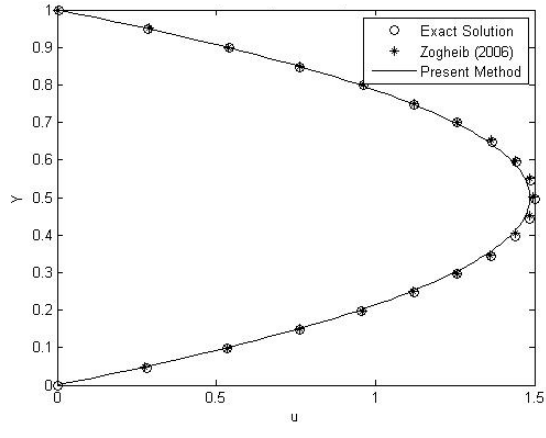

Figure 3: Fully developed velocity profile.

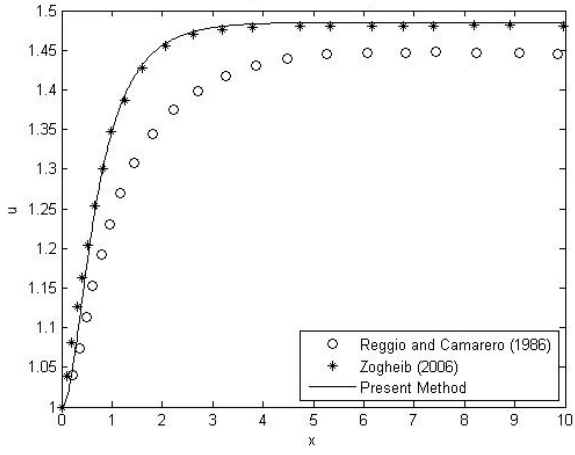

Figure 4: Centreline velocity for Re = 50.

5. Biomagnetic Flow in a Channel

Having just established an agreement with the benchmark problem, we consider here a biomagnetic flow in a channel that is prescribed with a spatially varying magnetic field. The biomagnetic fluid flow is considered taking place between two parallel plates (channel). From Figure 5, the length of the plates is L and the distance between them is D. The channel is modeled such that $L/D = 10$. The flow at the entrance is assumed to be fully developed. The flow is subjected to a magnetic source which is placed at $(a,b) = (2.5,-0.5)$. In medical application, the magnetic source is focused onto the region of the tumor[4-6] as part of the MDT technique.

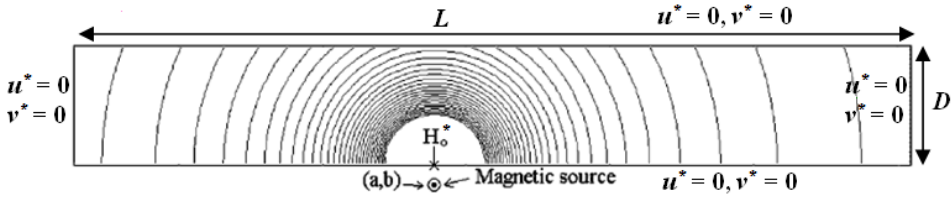

Figure 5: Flow domain and contours of the magnetic field intensity H.

The formulae for magnetic field intensity is given[11] by

$$H^*(x^*, y^*) = \left[H_x^{*2} + H_y^{*2} \right]^{1/2} = \frac{\gamma}{2\pi} \frac{1}{\sqrt{(x^* - a)^2 + (y^* - b)^2}}. \quad (9)$$

The intensity of the magnetic field varies radially in accordance to the proximity of the point source to the channel. The magnetic strength decreases considerably in a nonlinear manner as one traverse away from the source. The weakening of the magnetic effect is shown by the consistent narrowness of the strength contour near the source that loosens at the inlet and outlet of the channel for instance.

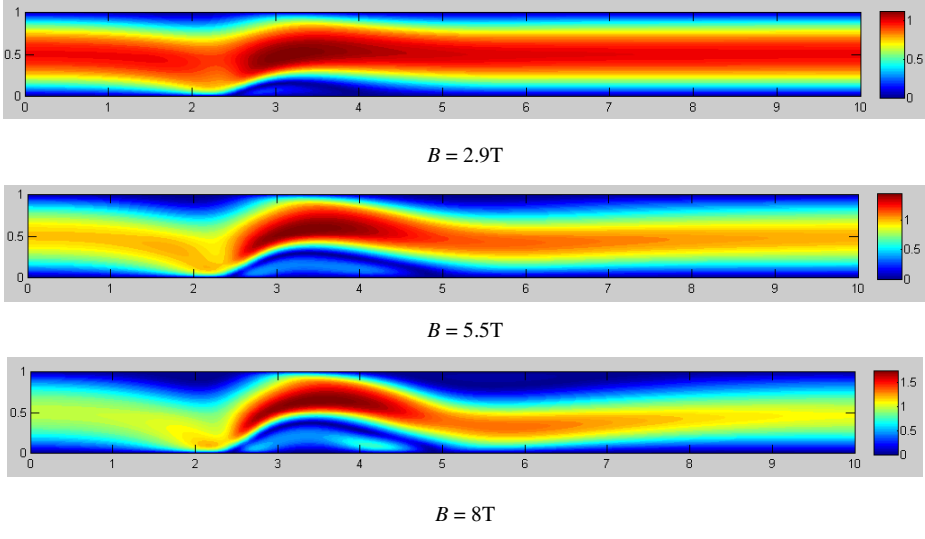

Figure 6: *U* velocity profiles for various magnetic effect.

In general, the presence of magnetic field appreciably influences the flow field. Figure 6 demonstrates the *U* velocity profiles of the biomagnetic flow for several magnetic effects. An increase in the magnetic strength *B* causes perturbation in the flow pattern and an elevation of maximum velocity along the flow direction. A vortex is arising near the lower plate where the magnetic source is placed. Therefore, blood flow recirculation may occur in this region. Observe also that the waviness of the velocity profile especially that near the magnetic source region has been increased. This is consistent with the enhancement of the flow vortex exerted by an increment of magnetic intensity.

Figure 7 shows the comparison of results computed by the present method and Ref. 16 for B = 8T for velocity profile at several x locations plotted transverse to the flow direction. Note that in absence of study of nature similar to the current model from literature, the comparison is made upon results from Ref. 16 which considered additional energy equation in their formulation. While having good agreement for all plots, a somewhat distorted profile with an unsymmetrical distribution is demonstrated in Figure 7(b) from the present method, indicating the sensitivity to the prescribed magnetic load. In addition, the profile peak computed from the present method is about 10% higher than that obtained from Ref. 16. The present model demonstrates somewhat lower velocity

peaks in Figures 7(d) and (e) in particular compared to those computed in Ref. 16. Both models capture the flow recirculation due to the existence of vortex in the lower half region of the channel as shown in Figures 7(c) and (d) which is consistent with the location of the magnetic source.

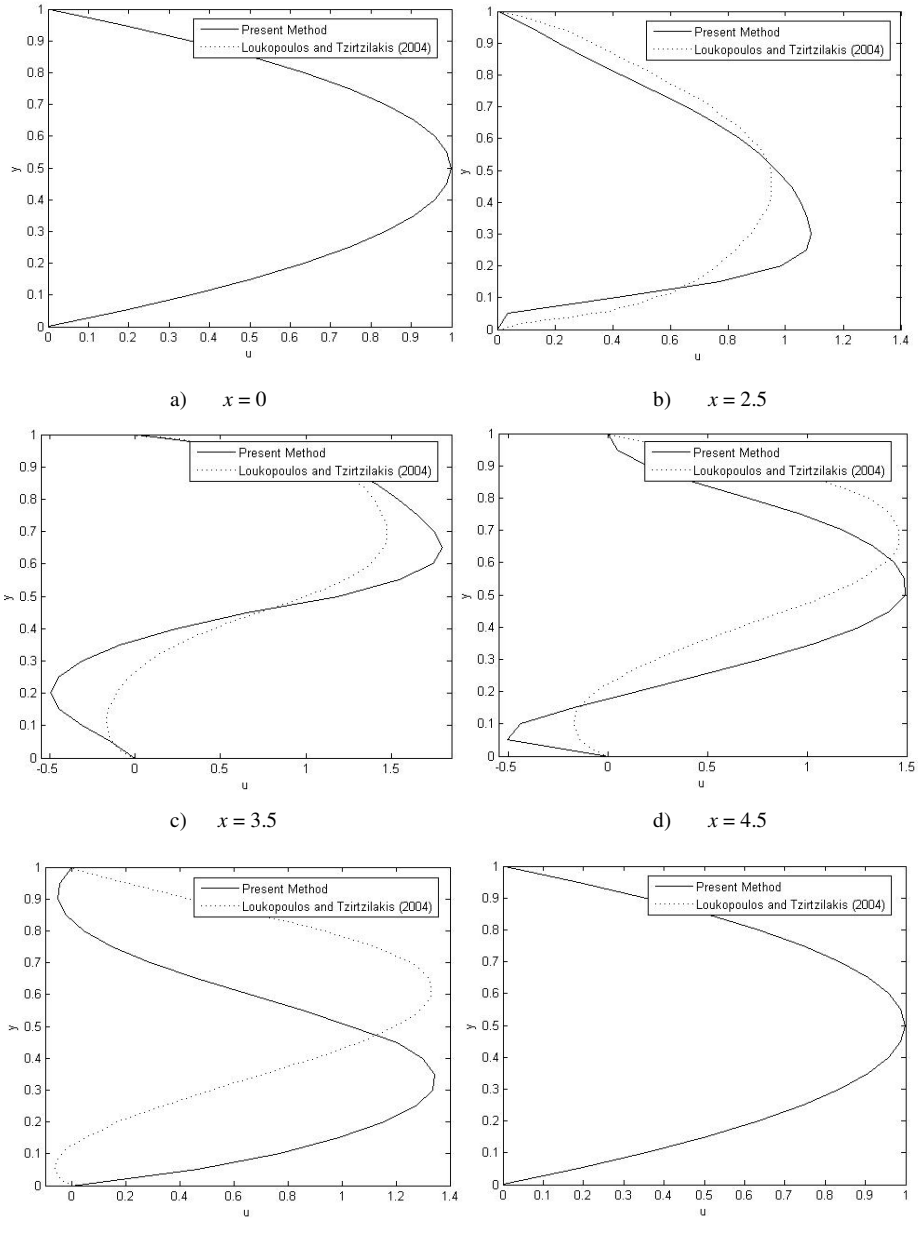

a) $x = 0$ b) $x = 2.5$

c) $x = 3.5$ d) $x = 4.5$

e) $x = 5.5$ f) $x = 10$

Figure 7: Comparison of velocity profiles with Ref. 16 for $B = 8$T.

6. Conclusions

A modified algorithm is presented for solving a biomagnetic fluid flow in a channel under the influence of a spatially varying magnetic field. The solution of the problem is obtained using a numerical technique based on the finite difference method. Results concerning the velocity indicates that the presence of magnetic field appreciably influence the flow field. Good agreements are observed for the present model in comparison to literature except for the cases where flows are slightly away from the magnetic source. The differences may arise from the absence of energy equation in the current formulation. Nonetheless, the present model captures the flow recirculation due to the existence of vortex near the magnetic source similar to that obtained in Ref. 16. In general, the existence of a magnetic field alters the behaviours blood flow considerably. Therefore, further numerical study is demanded especially in characterizing the blood flow in accordance to single and multiple simultaneous magnetic effects before a clinical procedure can be conducted.

Acknowledgments

We would like to thank FRGS Vot 78345, UniMAP and SLAI (JPA) for financial support.

References

1. Y. Haik, V. Pai and C. J. Chen, Biomagnetic Fluid Dynamics, in *Fluid Dynamics at Interfaces*, edited by W. Shyy and R. Narayanan (Cambridge University Press, Cambridge, 1999), p. 439.
2. E. K. Ruuge and A. N. Rusetski, *J. Magn. Magn. Mat*. **122**, 335 (1993).
3. J. Plavins and M. Lauva, *J. Magn. Magn. Mat*. **122**, 349 (1993).
4. C. Alexiou *et al*., *Cancer Res.* **60**, 6641 (2000).
5. C. Alexiou *et al*., *J. Magn. Magn. Mat*. **252**, 363 (2002).
6. C. Alexiou *et al*., *Eur. Biophys J.* **35**, 446 (2006).
7. M. O. Aviles *et al*., *J. Magn. Magn. Mat*. **293**, 605 (2005).
8. J. A. Ritter *et al*., *J. Magn. Magn. Mat*. **280**, 184 (2004).
9. J. W. Haverkort, S. Kenjeres and C. R. Kleijn, *Ann. Biomed. Eng*. **37**, 12 (2009).
10. R. E. Rosensweig, *Ferrohydrodynamics*. (Cambridge University Press, Cambridge, 1985).
11. E. E. Tzirtzilakis, *Phys. Fluids* **17**, 077103 (2005).
12. G. W. Sutton and A. Sherman, *Engineering Magnetohydrodynamics*. (McGraw-Hill, New York, 1965).
13. S. Kenjeres, *Int. J. Heat Fluid Flow* **29**, 752 (2008).
14. P. Jehenson *et al*., *Radiology* **166**, 227 (1988).
15. T. S. Tenforde, *Automedica* **14**, 271 (1992).
16. V. C. Loukopoulos and E. E. Tzirtzilakis, *J. Eng. Sci.* **42**, 571 (2004).
17. E. E. Tzirtzilakis, *Comm. Num. Meth. Eng*. **24**, 683 (2008).
18. E. E. Tzirtzilakis, *Pysica D* **237**, 66 (2008).
19. Y. Haik, C. J. Chen and J. Chatterjee, *J Visualization* **5**, 187 (2002).
20. S. A. Khashan and Y. Haik, *Phys. Fluids* **18**, 113601 (2006).
21. B. Zogheib, *Velocity-Pressure Coupling in Finite Difference Formulations for the Navier-Stokes Equations*. (Windsor, Ontario, Canada, 2006).

22. H. K. Versteeg and W. Malalasekera, *An Introduction to Computational Fluid Dynamics: The Finite Volume Approach*. (Pearson, UK, 1995).
23. C. Midya *et al*., *J. Fluid Eng*. **125**, 952 (2003).
24. J. H. Ferziger and M. Peric, *Computational Methods for Fluid Dynamics*, 3rd edn. (Springer, USA, 2002).
25. M. Reggio and R. Camarero, *Num. Heat Transfer A* **10**, 131. (1986).